

Pulse-by-pulse measurements of dynamic retention and deposition in NSTX

C.H. Skinner^{a,*}, H.W. Kugel^a, A.L. Roquemore^a, R. Maingi^b, W.R. Wampler^c

^a Princeton Plasma Physics Laboratory, P.O. Box 451, Princeton, NJ 08543, USA

^b Oak Ridge National Laboratory, Oak Ridge, TN 37831, USA

^c Sandia National Laboratory, Albuquerque, NM 87185, USA

Abstract

Three quartz crystal microbalances have been deployed in NSTX to measure deposition/erosion in plasma shadowed areas at the upper and lower divertor and outboard midplane. These show a complex pattern of material gain and loss. At the time of a plasma discharge a transient increase in mass of order $\sim 0.1 \mu\text{g cm}^{-2}$ is observed that decays in the interpulse period to a level either higher, lower or similar to that prior to the discharge. The first discharge of the day always shows a long term step-up in mass. Some correlations of mass gain with plasma duration, stored energy, and change in the plasma shape are observed. Following a days plasma operations, a slow decay in mass is observed. The results are interpreted in terms of dynamic retention and erosion/deposition.

© 2007 Elsevier B.V. All rights reserved.

PACS: 52.40.Hf; 52.90.+z

Keywords: Amorphous films; Desorption; Erosion and deposition; NSTX; Retention

1. Introduction

Control of tritium inventory is a pivotal issue for the successful development of fusion energy [1,2]. This area has high risk and high consequences for ITER's burning plasma goals because (i) experience on TFTR and JET has shown a fractional tritium retention that would be unacceptable in ITER (ii) tritium removal technology of suitable speed and efficiency has not yet been proven on a tokamak

[3] and (iii) predictive models of retention have not yet been validated in tokamak experiments [4,5]. Once ITER's tritium inventory approaches a limit to be set by nuclear licensing authorities, DT plasma operations will cease until the inventory is reduced. The challenge in developing a physics understanding of tritium retention lies in the disparate range of phenomena involved from solid state physics, surface physics, hydrocarbon chemistry, and plasma physics, coupled with the difficulty of diagnosing the composition and characteristics of the plasma facing surfaces that are created in a working tokamak.

Hydrogen isotopes are absorbed by plasma facing components during a tokamak discharge

* Corresponding author. Tel.: +1 609 243 2214; fax: +1 609 243 2665.

E-mail address: cskinner@pppl.gov (C.H. Skinner).

and some of this gas is released following the discharge. This is known as dynamic retention and is studied by measuring the global particle balance of gas fueling and exhaust [6,7]. This data set has time resolution but no spatial information on the location of the surfaces involved. Hydrogen can also be codeposited with eroded B, Be or C and the layer growth results in a continuous increase of the in-vessel hydrogen isotope inventory [8–10]. These deposits are measured by surface analysis of tiles retrieved from tokamaks. In contrast to the gas balance data, this data set has well-defined spatial resolution but no time resolution within a particular operational campaign. Quartz crystal microbalances (QMBs) are used to monitor the growth of thin films and have the advantage of both a well defined spatial location and time resolution. Their spatial coverage is limited as they cannot be used in high heat flux areas, also they cannot resolve changes during a discharge. Nonetheless they offer valuable data on material gained and lost from discharge to discharge at well defined locations in low heat flux areas and these measurements can be used to challenge models of dynamic retention and erosion/deposition and advance a predictive understanding of processes occurring at the plasma boundary and wall.

Previous quartz crystal microbalance measurements of the growth of thin films in the lower divertor of Asdex-U have shown the role of neutrals and of a parasitic plasma [11]. On JET the deposition was found to depend on the distance from the QMB to the divertor strike point [12]. Film deposition at ≈ 30 nm/h was measured with a QMB on TEXTOR [13]. On the National Spherical Torus Experiment (NSTX) two QMBs were previously installed in a location 0.77 m from the plasma that mimicked a typical diagnostic mirror [14]. Interestingly, a slow rise in deposition in the inter-pulse period was observed and it was suggested that this may be related to the condensation of polymer-like films after each discharge.

2. NSTX experimental setup and calibration

The National Spherical Torus Experiment is aimed at exploring the physics of high beta and high confinement in a low aspect ratio device [15]. Plasma facing components that are in contact with the plasma are protected by a combination of graphite and carbon fiber composite tiles. The surface temperature of the tiles at the outer divertor strike point can increase to 250–500 °C during a

high power discharge [16]. For the 2005/2006 NSTX campaigns the QMBs were positioned in 7 cm wide slots in the upper and lower outer divertor at Bay H, 7 cm back from the tile surface. A third QMB was installed at the outer midplane at Bay I, 10 cm out-board of the surface of the nearby neutral beam armor (see Fig. 1). Each microbalance contained a quartz crystal that oscillated at a frequency close to 6 MHz, the precise frequency depending on the deposited mass and crystal temperature. The oscillation frequency was measured with a Modelock™ system that is immune to mode hopping and was acquired every 2 s by a RS232 link. The manufacturer [17] specifies a measurement precision of 0.1 Hz or 0.012 nm for unit density per 0.25 s sampling time. The film mass was calculated from the frequency constant of the AT cut crystal that was provided by the manufacturer and was in good agreement with independent measurements by nuclear reaction analysis [14]. For estimation of the film thickness a nominal density of 1.6 g/cm³ was assumed. A 90% transmission mesh covered the crystal and the results below include a $\times 1.1$ correction factor. An intermittent in-vessel fault in the Bay I QMB limited the midplane data coverage.

A type K thermocouple was attached to each QMB crystal housing to track the temperature.

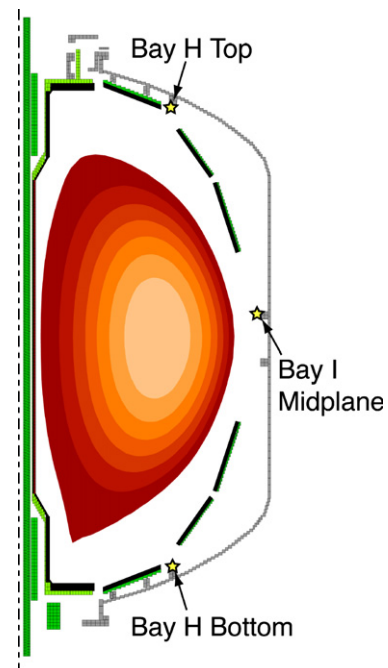


Fig. 1. Cross section of half the NSTX vessel with center column, divertor and passive plates. The QMB locations are denoted by stars.

Monitoring the temperature drift and associated QMB frequency changes over weekend periods without plasmas showed that the change in crystal frequency for a temperature change of $0.1\text{ }^{\circ}\text{C}$ was equivalent to a deposition of $+0.006\text{ }\mu\text{g}/\text{cm}^2$. In the following figures the mass after subtraction of temperature induced frequency changes is plotted. It is possible for the thermocouple and crystal temperatures to differ for a short time after transient heating by a plasma discharge. The time scale for thermal equilibration was measured at atmospheric pressure on a separate but identical QMB by bringing a hot soldering iron into contact with the front of the crystal housing for 20 s causing a transient crystal frequency decrease and thermocouple temperature rise. The temperature corrected thickness recovered its original value within 1–2 min after the heat pulse indicating that, after temperature correction, the thickness could be reliably measured by the QMB 2 min after a plasma discharge.

A unexpected sensitivity of the QMB to optical radiation was found. When either a halogen lamp, a ‘Spectroline’ Hg UV lamp, or soldering iron was placed within a few cm of a fresh uncoated crystal at atmospheric pressure the thickness indicated by the readout decreased by a few nm as seen in Fig. 2. No change was observed when the light was blocked by Al foil. When the radiation source was removed the crystal readout recovered its original thickness. This effect is opposite in sign to any thermal heating process and reveals a surprising QMB sensitivity to strong optical, UV and IR radiation. This will not affect NSTX measurements

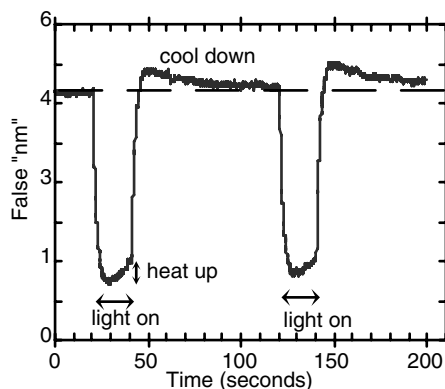


Fig. 2. Change in apparent ‘thickness’ indicated by the QMB readout on illumination of the quartz crystal by a halogen lamp at the times indicated. A sensitivity to light is apparent. Thermal heating and cooling of the crystal by the lamp are also evident but are of opposite sign.

taken outside of the time of the plasma discharge. Glow discharges alone had a negligible effect ($<0.1\text{ nm}$) on the Bay H top and bottom QMBs but a transient (0.5 nm) effect on the Bay I midplane QMB could be seen at the time of glow.

Nuclear reaction analysis was performed to determine the composition of layers deposited on crystals exposed to 2005 plasmas. A $2.5\text{ MeV }^3\text{He}$ beam was used and the resulting protons from the $^{12}\text{C}(^3\text{He},\text{p})^{14}\text{N}$, $^{11}\text{B}(^3\text{He},\text{p})^{13}\text{C}$, and $^2\text{H}(^3\text{He},\text{p})^4\text{He}$ reactions were counted. The average atomic composition of the deposited material was $\sim 58\%$ carbon, $\sim 27\%$ deuterium and $\sim 15\%$ boron. Analysis was also performed on 24 Si witness coupons that were distributed poloidally and toroidally in NSTX. ^7Li was measured by the exothermic nuclear reaction $^7\text{Li}(\text{p},^4\text{He})^4\text{He}$ as Li pellets had been used on two occasions. The average coupon composition was $\sim 47\%$ carbon, 32% deuterium and 21% boron and 0.1% Li. Oxygen was excluded from the analysis as oxygen was present in the quartz substrates and boron can react with atmospheric oxygen. The deposition pattern peaked at the outer midplane.

Before plasma operations the vessel was baked at $350\text{ }^{\circ}\text{C}$ for several days. During this time room temperature air was blown through the QMB cooling lines to limit the temperature rise. The 2005 campaign lasted 17 run weeks during which time the vessel was boronized using a glow discharge of trimethyl boron $\text{B}(\text{CD}_3)_3$ and helium [18] for five periods of 2–3 h and four periods of 20–30 min. The deposition rate during boronization was measured to be $0.036\text{ nm}/\text{min}$ at Bay H top, $0.019\text{ nm}/\text{min}$ at Bay H bottom and $0.90\text{ nm}/\text{min}$ at Bay I midplane for an assumed density of $1.6\text{ g}/\text{cm}^3$. The high midplane deposition is attributed to the proximity of the $\text{B}(\text{CD}_3)_3$ gas inlet and glow discharge electrodes that are also close to the midplane.

3. QMB mass gain and loss in NSTX

The QMBs show a complex pattern of mass gain and loss. Fig. 3(a) shows 24 h of data recorded from the Bay H bottom QMB on 10 May 2005. Plasma operations were from 10:30 to 19:00 h. The discharges are apparent in transient excursions and Fig. 3(b) shows the first four discharges on an expanded time scale. The most striking feature is a large step-up in mass with the first discharge of the day. Both the Bay H top and bottom QMBs show a $0.35\text{ }\mu\text{g}/\text{cm}^2$ transient rise, that relaxes to a level $0.24\text{ }\mu\text{g}/\text{cm}^2$ higher than the level before the

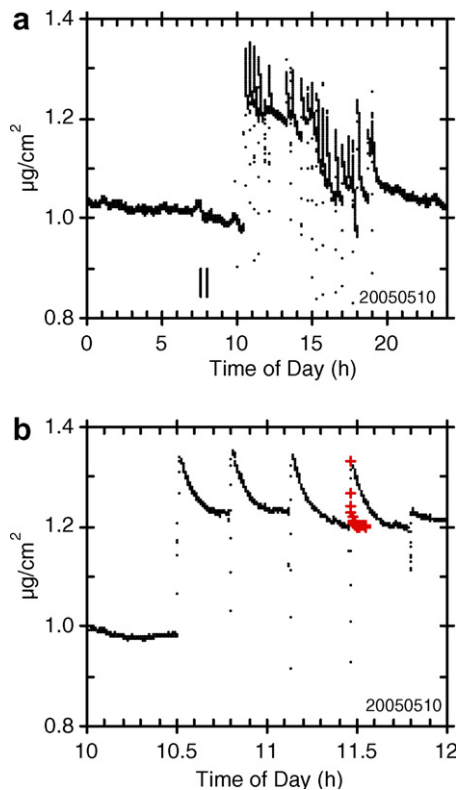


Fig. 3. (a) Change in mass recorded by the Bay H bottom QMB on 10 May 2005. The time of He glow discharge is marked by vertical lines. (b) Expanded plot of the first four discharges of the same day (115647...) showing the large step-up on the first shot. For comparison the QMB thermal equilibration response has been scaled and plotted (+) over the trace for the fourth discharge showing that the post shot decay is not a temperature effect. The Y-axis zero is arbitrary.

discharge. The next three discharges have similar plasma parameters (LSN, $I_p \approx 900$ kA or 1 MA, 4 MW neutral beam injection (NBI), peak $T_e \approx 1$ keV, max $N_{el} \approx 6 \times 10^{15} \text{ cm}^{-2}$) but show only a $0.12 \mu\text{g}/\text{cm}^2$ transient rise that decays back to the prior level without a significant longer term change in mass. This decay time exceeds the 1–2 min QMB thermal equilibration time (Section 2) shown overlaid on the fourth discharge. A large step up in layer mass is universally observed on the first discharge of the day whatever its plasma parameters. For example a first discharge of the day without NBI (115476) also showed a $0.04 \mu\text{g}/\text{cm}^2$ step up on Bay H top and bottom QMBs. One common factor is that a 30 min He glow discharge almost always precedes the first discharge of the day. However, on 9 March 2006 the first two discharges of the day were deliberately run without any prior He GDC and these also showed a large step up in layer

thickness, a remarkable $1.3 \mu\text{g}/\text{cm}^2$ for the Bay I midplane QMB. It appears that there is an overnight change in the condition of the plasma facing surfaces that always causes strong mass gain on the QMBs on the first discharge of the day. Subsequent discharges are more variable and show transient deposition with or without a change in asymptote in the interpulse period. The decline in mass following a discharge can be tracked after a day's plasma operations when there is no interpulse He glow discharge and the vessel is pumped solely by the turbo pumps with the NBI valve closed. This decline in mass tracks the time dependence of the decrease in the vessel base pressure which residual gas analysis shows is dominantly deuterium.

The above data are qualitatively consistent with mass gain through transient uptake of deuterium from the plasma followed by outgassing, a process known as dynamic retention [7]. The four discharges in Fig. 3(b) have a total fueling from gas puff and neutral beam injection of 5×10^{21} D atoms or 0.017 g of D. If spread uniformly over the NSTX vacuum vessel area of 40.66 m^2 this would correspond to a mass of $0.04 \mu\text{g}/\text{cm}^2$ whereas the QMBs show an initial mass gain of $0.35 \mu\text{g}/\text{cm}^2$. It appears that dynamic retention is concentrated in plasma shadowed regions that from the QMB measurements represent about 10% of the total vessel area. The decline in mass measured by the QMBs over 1 h after the last discharge of the day may also be compared with the amount of gas pumped out over the same time (integral of vessel pressure \times pumping speed). Simple extrapolation of the QMB mass loss to the whole vessel area results in more than an order of magnitude higher mass loss than the mass of deuterium pumped, also indicating that the dynamic retention is concentrated over a small fraction of the vessel surface.

Fig. 4 shows the QMB mass on 14 June 2005, a day that began with high performance neutral beam heated lower single null plasmas followed by LSN ohmic discharges. The ohmic discharges generally show much less transient mass gain and steps up or down in the asymptotic level after a discharge with one exception, the first ohmic discharge (116322) at 14.16 h. This discharge was significantly different in shape with lower triangularity than the preceding one. A change in QMB asymptote often correlates with a change in plasma shape that exposes a previous deposition area to erosion. An enhanced chemical sputtering yield for fresh re-deposits has been postulated in Ref. [19]. Some of

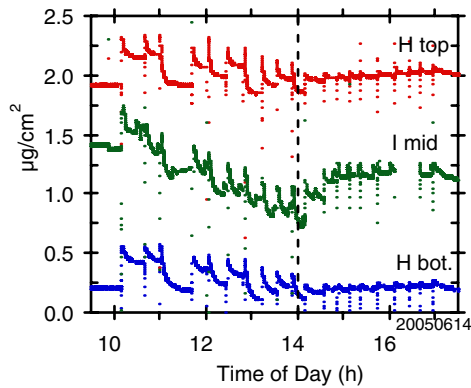


Fig. 4. Mass gain and loss of the QMBs at Bay H bottom, Bay I midplane and Bay H top on 14 June 2005. The dashed line marks a change from NBI heated to ohmic discharges. The Y-axis zero is arbitrary.

the discharges in the first part of the day had high stored energy and high duration (up to 1.6 s). IR thermography of a tile adjacent to the Bay H bottom QMB shows a surface temperature rise increasing from 5 °C for a short ohmic discharge to 30 °C for a long pulse NBI discharge. Additional frequency excursions synchronous with the interpulse He glow discharge are seen in the trace for the Bay I midplane QMB. The asymptotic value of the decay after a discharge is often not reached before the subsequent discharge. Fig. 5 shows a plot of mass change from 1 min before a discharge to 1 min before the next discharge against the integral

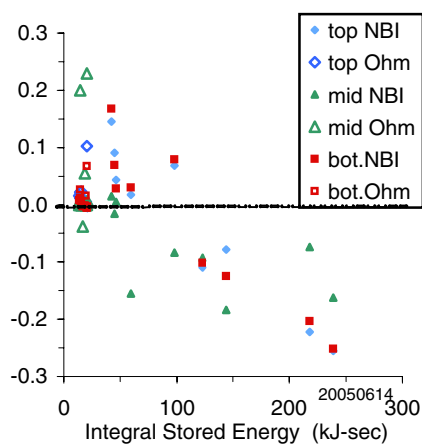


Fig. 5. Change in mass from 1 min before a discharge to 1 min before next discharge plotted vs. the integral of stored energy vs. time. The legend denotes the location of the QMB and whether NBI or solely ohmic heating was used.

of the stored energy. Some correlation of mass gain/loss with stored energy is apparent.

The net effect of plasma erosion and deposition is evident over the longer term. The mass gain/loss for the Bay H bottom and top QMBs from 23 April to 13 September was $-0.26 \mu\text{g}/\text{cm}^2$ and $2.57 \mu\text{g}/\text{cm}^2$ respectively. After subtraction of the mass gain from boronization, the net change was $-4.5 \mu\text{g}/\text{cm}^2$ and $0.5 \mu\text{g}/\text{cm}^2$, respectively. This corresponds to an average of $-0.0028 \mu\text{g}/\text{cm}^2/\text{discharge}$ and $0.0003 \mu\text{g}/\text{cm}^2/\text{discharge}$ or $-0.0051 \mu\text{g}/\text{cm}^2/\text{s}$ and $0.0006 \mu\text{g}/\text{cm}^2/\text{s}$ for the QMBs at Bay H bottom and top respectively.

In summary the mass gain/loss of the QMBs in plasma shadowed regions at the outer divertor and vessel wall show a complex time history consistent with dynamic retention of deuterium in a small fraction of the vessel area. Some correlation with plasma position and the integral of stored energy was found. Long term net erosion and deposition is small at the location of the QMBs.

Acknowledgements

The authors thank T. Holoman, D. Labrie, P. Roney and the NSTX team for technical assistance. We thank R. Kaita for assistance with the QMB thermal calibration. This work was funded by US DOE Contract No. DE-AC02-76CH0307.

References

- [1] G. Federici et al., Nucl. Fus. 41 (2001) 1967.
- [2] G. Federici, Phys. Scr. T 124 (2006) 1.
- [3] C.H. Skinner et al., Phys. Scr. T 111 (2004) 92.
- [4] J.N. Brooks et al., J. Nucl. Mater. 313–316 (2003) 424.
- [5] C.H. Skinner, G. Federici, Phys. Scr. T 124 (2006) 18.
- [6] G. Haas et al., J. Nucl. Mater. 226–229 (1999) 1065.
- [7] P. Andrew, M. Pick, J. Nucl. Mater. 220–222 (1995) 601.
- [8] W. Jacob, J. Nucl. Mater. 337–339 (2005) 839.
- [9] M. Mayer et al., J. Nucl. Mater. 290–293 (2001) 381.
- [10] C.H. Skinner et al., J. Nucl. Mater. 290–293 (2001) 486.
- [11] V. Rhode et al., J. Nucl. Mater. 337–339 (2005) 847.
- [12] H.G. Esser et al., J. Nucl. Mater. 337–339 (2005) 84.
- [13] J. von Seggern et al., J. Nucl. Mater. 313–316 (2003) 439.
- [14] C.H. Skinner et al., J. Nucl. Mater. 337–339 (2005) 129.
- [15] S.M. Kaye et al., Nucl. Fus. 45 (2005) 168.
- [16] D.A. Mastrovito et al., Rev. Sci. Instrum. 74 (2003) 5090.
- [17] Leybold Infinicon, Two Technology Place, East Syracuse, NY; model XTM2P/11231000.
- [18] C.H. Skinner et al., Nucl. Fus. 42 (2002) 329.
- [19] A. Kirschner et al., J. Nucl. Mater. 328 (2004) 62.